CustomSketching: Sketch Concept Extraction for Sketch-based Image Synthesis and Editing

Chufeng Xiao, Hongbo Fu✉
School of Creative Media, City University of Hong Kong
chufengxiao@outlook.com, fuplus@gmail.com

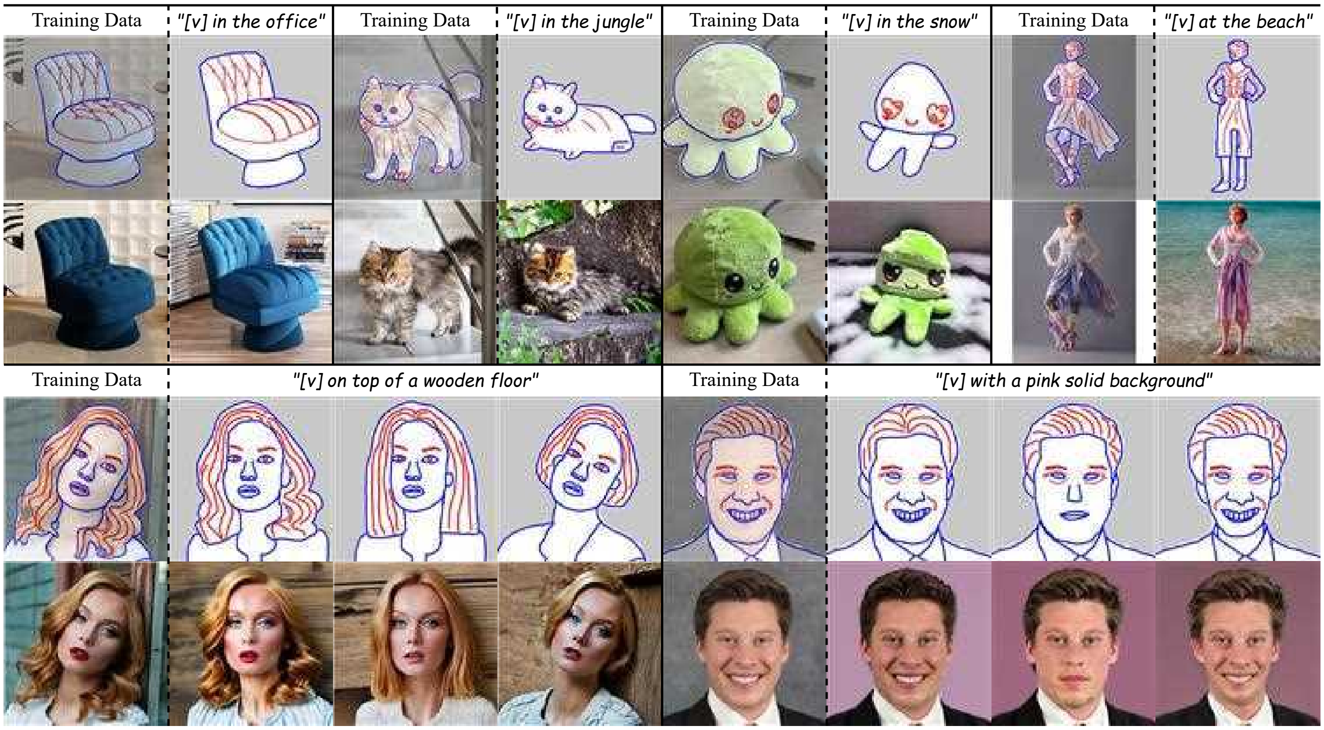

Figure 1. Given one or several sketch-image pairs as training data, our *CustomSketching* can learn a novel sketch concept into a text token $[v]$ and specific sketches. We decompose a sketch into shape lines (blue strokes) and detail lines (red strokes) to reduce the ambiguity in a sketch. Users may input a text prompt and a dual-sketch to re-create or edit the concept at a fine-grained level.

Abstract

Personalization techniques for large text-to-image (T2I) models allow users to incorporate new concepts from reference images. However, existing methods primarily rely on textual descriptions, leading to limited control over customized images and failing to support fine-grained and local editing (e.g., shape, pose, and details). In this paper, we identify sketches as an intuitive and versatile representation that can facilitate such control, e.g., contour lines capturing shape information and flow lines representing texture. This motivates us to explore a novel task of sketch concept extraction: given one or more sketch-image pairs, we aim to extract a special sketch concept that bridges the correspondence between the images and sketches, thus enabling sketch-based image synthesis and editing at a fine-grained level. To accomplish this, we introduce CustomSketching, a two-stage framework for extracting novel sketch concepts. Considering that an object can often be depicted by a contour for general shapes and additional strokes for internal details, we introduce a dual-sketch *representation to reduce the inherent ambiguity in sketch depiction. We employ a shape loss and a regularization loss to balance fidelity and editability during optimization. Through extensive experi-*

ments, a user study, and several applications, we show our method is effective and superior to the adapted baselines.

1. Introduction

The recent advent of large text-to-image (T2I) models [44, 47, 49] has opened up new avenues for image synthesis given text prompts. Based on such models, personalization techniques like [21, 31, 48] have been proposed to learn novel concepts on unseen reference images by fine-tuning the pre-trained models. Users can employ text prompts to create novel images containing the learned concepts in diverse contexts by leveraging the significant semantic priors of these powerful generative models.

However, the existing personalization methods fail to accurately capture the spatial features of target objects in terms of their geometry and appearance. This limitation arises due to their heavy reliance on textual descriptions during the image generation process. While some following works like [3, 15] have attempted to address this issue by incorporating explicit masks or additional spatial image features, they are still limited to providing precise controls and local editing on fine-grained object attributes (e.g., shape, pose, details) for the target concept solely through text.

To achieve fine-grained controls, sketches can serve as an intuitive and versatile handle for providing explicit guidance. T2I-Adapter [36] and ControlNet [70] have enabled the T2I models to be conditioned on sketches by incorporating an additional encoder network for sketch-based image generation. Such conditional methods perform well when an input sketch depicts the general contour of an object (e.g., the blue strokes in Figure 2 (b)). However, we observed they struggle to interpret and differentiate other types of sketches corresponding to specific local features in realistic images. As illustrated in Figure 2, these methods fail to correctly interpret detail lines for clothing folds and flow lines for hair texture (the red strokes in (b)). The primary reason behind the issue is that the sketch dataset used to train the conditional networks [36, 70] is inherently ambiguous since it is generated automatically through edge detection on photo-realistic images. Consequently, directly incorporating a pre-trained sketch encoder with personalization techniques proves challenging when attempting to customize a novel concept guided by sketches.

Based on the aforementioned observation, we propose a novel task of sketch concept extraction for image synthesis and editing to tackle the issue of sketch ambiguity. The key idea is to empower users to define personalized sketches corresponding to specific local features in photo-realistic images. Users can sketch their desired concepts by first tracing upon one or more reference images and then manipulating the learned concepts by sketching, as shown in Figure 1.

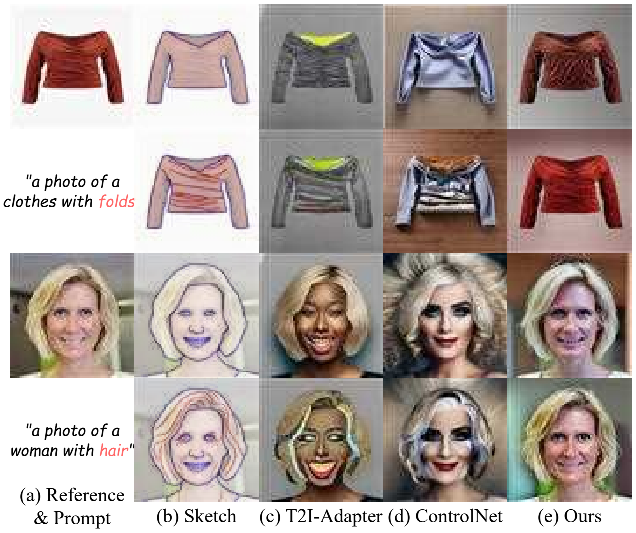

Figure 2. Given a text prompt (a, bottom) and a sketch (b) depicting specific semantics (e.g., clothing folds and hair), T2I-adapter (c) and ControlNet (d) could not correctly interpret the out-of-domain sketch types, while our method can extract such a novel sketch concept and reconstruct the reference image (a, top). Note that the reference image is not used by (c) and (d), and their results are for reference only.

To achieve sketch-based editability and identity preservation, we propose a novel personalization pipeline called *CustomSketching* for extracting sketch concepts. This pipeline is built upon a pretrained T2I model and incorporates additional encoders to extract features from the sketch input. Since a single image may exhibit diverse local features corresponding to different types of sketches, we employ a dual-sketch representation via two sketch encoders to decouple shape and detail depiction. Our pipeline consists of two stages: in Stage I, we optimize a textual token for global semantics but freeze the weights of the sketch encoders; in Stage II, we jointly fine-tune the weights of the sketch encoders and the learned token to reconstruct the reference images in terms of local appearance and geometry. To prevent overfitting, we perform data augmentation and introduce a shape loss for sketch-guided shape constraint and a regularization loss for textual prior preservation.

To the best of our knowledge, our method is the first work to extract sketch concepts using large T2I models, thus providing users with enhanced creative capabilities for editing real images. To evaluate our method, we collect a new dataset including sketch-image pairs and the edited sketches, where each sketch comprises a dual representation. Through qualitative and quantitative experiments, we demonstrate the superiority and effectiveness of *CustomSketching*, compared to the adapted baselines. Given the absence of a definitive metric to measure the performance of image editing, we conduct a user study to gather user insights and feedback. Additionally, we showcase several applications enabled by our work.

The contributions of our work can be summarized as follows. 1) We propose the novel task of sketch concept extraction. 2) We introduce a novel framework that enables a large T2I model to extract and manipulate a sketch concept via sketching, thereby improving its editability and controllability. 3) We create a new dataset for comprehensive evaluations and demonstrate several sketch-based applications enabled by *CustomSketching*.

2. Related Work

Text-to-Image Synthesis and Editing. Text-to-image generation has made significant strides in recent years, achieving remarkable performance. Early works [45, 64, 67–69] employed RNN [17, 27] and GANs [6, 24, 29] to control image generation, processing, and editing in specific scenarios, such as human faces [62], fashion [33], and colorization [73]. These works rely on well-prepared datasets tailored to the target scenarios, posing a bottleneck in dataset availability. To alleviate this limitation, subsequent studies [1, 5, 19, 22, 34, 39] adopted CLIP [43], a large language-image representation model based on Transformer [56], to align image-text features and achieve robust performance in text-driven image manipulation tasks. Nonetheless, these approaches are still confined to limited domains, challenging their extension to other domains.

The emergence of diffusion models [20, 26, 44, 47, 52, 53] trained with large-scale image-text datasets allows for universal image generation from open-domain text, surpassing previous works based on GANs. Leveraging the power of diffusion models, several approaches have been proposed to manipulate images globally using text [7, 8, 18, 30, 55] and locally using masks [37, 40, 60]. For example, Mokady et al. [35] proposed an inversion method that first inverts a real image into latent representations, given which the method enables text-based image editing (e.g., changing local objects or modifying global image styles) by manipulating cross-attention maps [25]. Blended Diffusion [2, 4] can merge an existing object into a real image. However, these approaches face challenges in modifying the fine-grained object attributes of real images due to the abstract nature of the text. Building upon Stable Diffusion [47], our method addresses this issue by incorporating sketches as an intuitive handle to manipulate real images. Inspired by [25], we introduce a shape loss that leverages cross-attention maps to provide guidance based on sketches.

Personalization Techniques. The personalization task is to produce image variations of a given concept in reference images. GAN-based methods for this task only focus on the same category (e.g., aligned faces) [38, 46] or on a single image [57], and thus could not manipulate images in a new context. Most recently, diffusion-based methods based on text-to-image models optimize a new [21] or rare [48] textual token to learn the novel concept and generate the concept in diverse contexts via text prompting. For fast personalization, many researchers [14, 15, 23, 28, 51, 61] introduce a prior encoder with local and global mapping to save optimization time. For multi-concept personalization, Avrahami et al. [3] fine-tuned a set of new tokens and the weights of a denoising network from a single image given masks, while Kumari et al. [31] optimized only several layers of the network based on a few images. Unlike these two methods, which need to fine-tune simultaneously the multi-concepts that are desired in generation, our method can separately extract sketch concepts for diverse targets and then work for multi-concept generation by plug-and-play without extra optimization (see Figure 8 (c)).

However, the existing personalization works do not allow precise control for novel concept generation and thus could not work for local or detailed editing (e.g., addition, removal, modification) of the learned concept. To address the issue, we introduce a new task of sketch concept extraction by optimizing sketch encoder(s) given one or more sketch-image pairs.

Sketch-based Image Synthesis and Editing. As an intuitive and versatile representation, sketch has been extensively explored to achieve fine-grained geometry control in realistic image synthesis and editing. For instance, Sangkloy et al. [50] utilized colored scribbles to depict geometry and appearance and synthesized images of various categories such as bedrooms, cars, and faces. Similarly, Chen and Hays [13] employed freehand sketches to learn shape knowledge for diverse objects. Chen et al. [11, 12] and Liu et al. [32] utilized line drawings for image synthesis, editing, and video editing of human faces. In SketchHairSalon [63], flow lines are used to represent unbraided hair, while contour lines depict braided hair. For local editing, a partial sketch has been adopted for minor image editing, e.g., FaceShop [42], Sketch2Edit [66], Draw2Edit [65]. Unlike the previous works that train dedicated networks for specific domains or limited object categories, our method is generic and few-shot, which can handle versatile sketches for image synthesis and editing using a pre-trained text-to-image model.

Recently, sketch-based text-to-image diffusion models have also been explored [16, 41, 59]. Voynov et al. [58] utilized sketches as a shape constraint for optimizing the latent map in a diffusion model, while T2I-Adapter [36] and ControlNet [70] are two concurrent works that train an external sketch encoder connected to a pre-trained diffusion model to enable sketch control. However, directly integrating these methods with personalization techniques may not accurately extract sketch concepts for all types of sketches (Figure 2), since the models [36, 70] are biased towards training data, specifically edge maps automatically detected

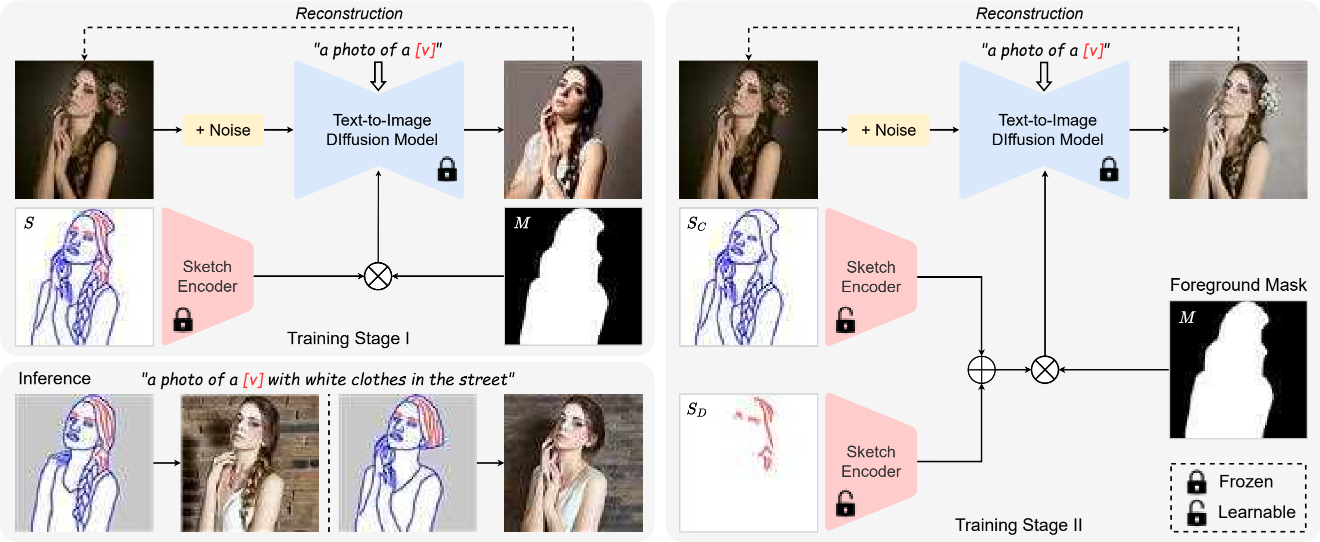

Figure 3. The pipeline of our *CustomSketching*, which extracts novel sketch concepts for fine-grained image synthesis and editing via a two-stage framework. During training, given one or a few sketch-image pairs, Stage I only optimizes a textual embedding of a newly added token $[v]$ to represent the global semantics of the reference image(s), while Stage II jointly fine-tunes the token and two sketch encoders to reconstruct the concept in terms of local appearance and geometry. We adopt a dual-sketch representation to differentiate shape lines S_C and detail lines S_D. During inference, users may provide a text prompt and a dual-sketch to manipulate the learned concept.

from images. We will establish this setup for the existing personalization methods as baselines to compare with our method, though we are the first to customize novel sketch concepts.

3. Method

Based on a pre-trained T2I diffusion model, our goal is to embed a new sketch concept into the model, enabling the synthesis and manipulation of diverse semantics in reference images through sketching and prompting (see Figure 1). To this end, we propose a novel framework, *CustomSketching*, which extracts a sketch concept from one or more reference images I and their corresponding sketches S. As illustrated in Figure 3, the framework comprises two training stages to reconstruct the reference image. During inference, users can flexibly control the generation of a target image that satisfies the context described by a text and faithfully reflects the input sketch in terms of geometry. In the following, we will describe the method details.

Two-stage Optimization. To leverage the robust textual prior of a large T2I model, following TI [21], we introduce a newly added textual token $[v]$ to capture global semantics while utilizing sketch representations through sketch encoder(s) to capture local features. Directly incorporating the personalization method [21] with a pre-trained encoder like [36] could not fully restore the local geometry and appearance of the target image (see the results by TI-E in Figure 4). It is because it fine-tunes merely textual embedding v for the token $[v]$. However, through joint optimization of the textual embedding and the weights of the sketch encoder(s), we encountered challenges in disentangling the global and local representations, resulting in unsatisfactory reconstruction (see Supp). To focus on learning separate features, inspired by [3], we adopt a two-stage optimization strategy. In Stage I, we optimize the textual embedding while freezing the weights of a pre-trained sketch encoder [36], establishing a pivotal initialization for the next stage. In Stage II, we jointly fine-tune the embedding and two sketch encoders to recover the target identity. Note that, in both stages, we freeze the denoising network of the pre-trained model to preserve its prior knowledge for editing.

Dual Sketch Representations. In Stage I, we fix the local features from sketches to guide the learning of the global textual embedding. To employ the prior knowledge of the sketch encoder [36], which was pre-trained on a large-scale sketch dataset, we input a binary sketch (where blue and red lines in Figure 3 are represented as black and the background as white) similar to the input used during pre-training. However, this single sketch representation inherently contains ambiguity since it combines the major contour sketch (blue lines, denoted as S_C) indicating the general shape with other minor types of sketches (red lines, denoted as S_D) capturing internal details (e.g., hair flow, clothes fold, wrinkles). This inherent ambiguity is the primary factor that biases the pre-trained sketch encoder [36, 70] towards general shape, as illustrated in Figure 2. Therefore, in Stage II, optimizing the weights of a sketch encoder using the single-sketch representation would still result in ambiguous image editing (see Section 4.2).

To address this issue, we propose using a dual-sketch representation that decomposes a given sketch S into two distinct types of sketches, namely S_C and S_D as mentioned above, for Stage II. Instead of merging S_C and S_D into a single map and feeding it into a single encoder (see Supp), we employ two separate sketch encoders to extract features corresponding to each type of sketch individually. This configuration enables us to capture more distinct and recognizable features for S_C and S_D, resulting in plausible performance in decomposing shape and details, compared to the setting of the single-sketch representation. The features extracted from both types of sketches are aggregated through summation before being injected into the pre-trained T2I model.

Masked Encoder. As our focus is sketching the concept in the foreground, the sketch map S often contains significant blank areas representing the background. Therefore, fine-tuning the sketch encoder(s) on the entire map would lead to overfitting the background regions not represented in the sketch, consequently undermining the text-guided editability of the T2I model (see Figure 7). To address it, we apply a foreground mask M to remove the background features extracted from the encoder(s). The foreground mask can either be generated automatically by filling a convex polygon following S_C, or be manually drawn by users. In summary, the sketch features are passed into the T2I model $\mathcal{F}_m$ along with a prompt p_v containing the token $[v]$ to derive the fused features $\mathcal{F}$. For Stage I, we denote it as:

$$\widehat{\mathcal{F}}^i = \mathcal{F}_e^i(S) \cdot M^i + \mathcal{F}_m^i(p_v), i \in \{1,2,3,4\}, \tag{1}$$

while for Stage II:

$$\widehat{\mathcal{F}}^i = (\mathcal{F}_c^i(S_C) + \mathcal{F}_d^i(S_D)) \cdot M^i + \mathcal{F}_m^i(p_v), \tag{2}$$

where $\mathcal{F}_e^i(S)$ is the i-th layer sketch feature extracted by the pre-trained encoder [36], while $\mathcal{F}_c^i(S_C)$ and $\mathcal{F}_d^i(S_D)$ are dual sketch representations from the fine-tuned encoders, and M_i is the resized mask fit to the feature size. We adopt four layers of the features as used in [36].

Loss Function. To optimize the sketch concept, which involves the embedding v and the weights of $\mathcal{F}_c$ and $\mathcal{F}_d$, we combine three types of losses for the text- and sketch-based problem. Firstly, we utilize a classic diffusion loss with the foreground mask M to reconstruct the target image regarding appearance and geometry. This loss encourages the optimization to concentrate on the foreground object depicted by the sketches, formulated as

$$\mathcal{L}_{rec} = \mathbb{E}_{z,t,v,\mathcal{F}_S,\epsilon}\left[\|\epsilon \cdot M - \epsilon_\theta(z_t, t, p_v, \mathcal{F}_S) \cdot M\|\right], \tag{3}$$

where $\mathcal{F}_S$ denotes the sketch features in the two stages, and ϵ_θ is the denoising network of the T2I model. At each optimization step, we randomly sample a timestep t from $[0, T]$ and add noise $\epsilon \sim \mathcal{N}(0,1)$ to the image latent z_0 to be z_t .

However, relying solely on the masked diffusion loss may not provide sufficient constraints to ensure the faithfulness between the sketch and the generated image. For example, certain parts depicted by the sketch would be lost, or unexpected elements would be produced in the generated results, as shown in Figure 6. Motivated by previous works [3, 10, 25] that leverage cross-attention maps of the T2I model to control the layout and semantics of the target, we propose a shape loss based on the cross-attention map of the token $[v]$. The shape loss $\mathcal{L}_{shape}$ comprises a foreground loss for guiding the concept shape to align with the sketch depiction via M, and a background loss for penalizing foreground pixels that violate the background region. We denote the shape loss as:

$$\mathcal{L}_{fg} = \|norm(A_\theta(z_t, v)) \cdot M - M\|, \tag{4}$$

$$\mathcal{L}_{bg} = mean(A_\theta(z_t, v) \cdot (1 - M)), \tag{5}$$

$$\mathcal{L}_{shape} = \mathcal{L}_{fg} + \mathcal{L}_{bg}, \tag{6}$$

where $A_\theta(z_t, v)$ is the cross-attention maps given the latent z_t and token $[v]$. $norm(\cdot)$ is to normalize the attention map to $[0, 1]$, while $mean(\cdot)$ computes the average attention value of background pixels.

In addition, the two-stage optimization may cause the fine-tuned embedding v to increase too large so that it overfits the reference shape, thus damaging the sketch editability (see Figures 6 & 7). We, therefore, introduce a regularization loss for the embedding via an $L2$ norm:

$$\mathcal{L}_{reg} = \|v\|. \tag{7}$$

In total, the loss function for the two stages is:

$$\mathcal{L}_{total} = \mathcal{L}_{rec} + \lambda_{shape}\mathcal{L}_{shape} + \lambda_{reg}\mathcal{L}_{reg}, \tag{8}$$

where we set the weights λ_{shape} as 0.01 and λ_{reg} as 0.001 empirically.

Implementation Details. To avoid the method overfitting a few training images, we adopt on-the-fly augmentation tricks (horizontal flip, translation, rotation) on the sketch-image pairs during optimization. Please find more implementation details in Supp.

4. Experiments

We have conducted extensive evaluations to quantitatively and qualitatively evaluate our method *CustomSketching*. We first show the comparisons between our method and the personalization baselines adapted to our proposed task. Then, we evaluate the effectiveness of our settings via an ablation study. We further conduct a perceptive user study on the edited results by the compared methods. In addition, we implement several applications based on our method to show the usefulness of the extracted sketch concepts. Please find more details, comparisons, and results in Supp.

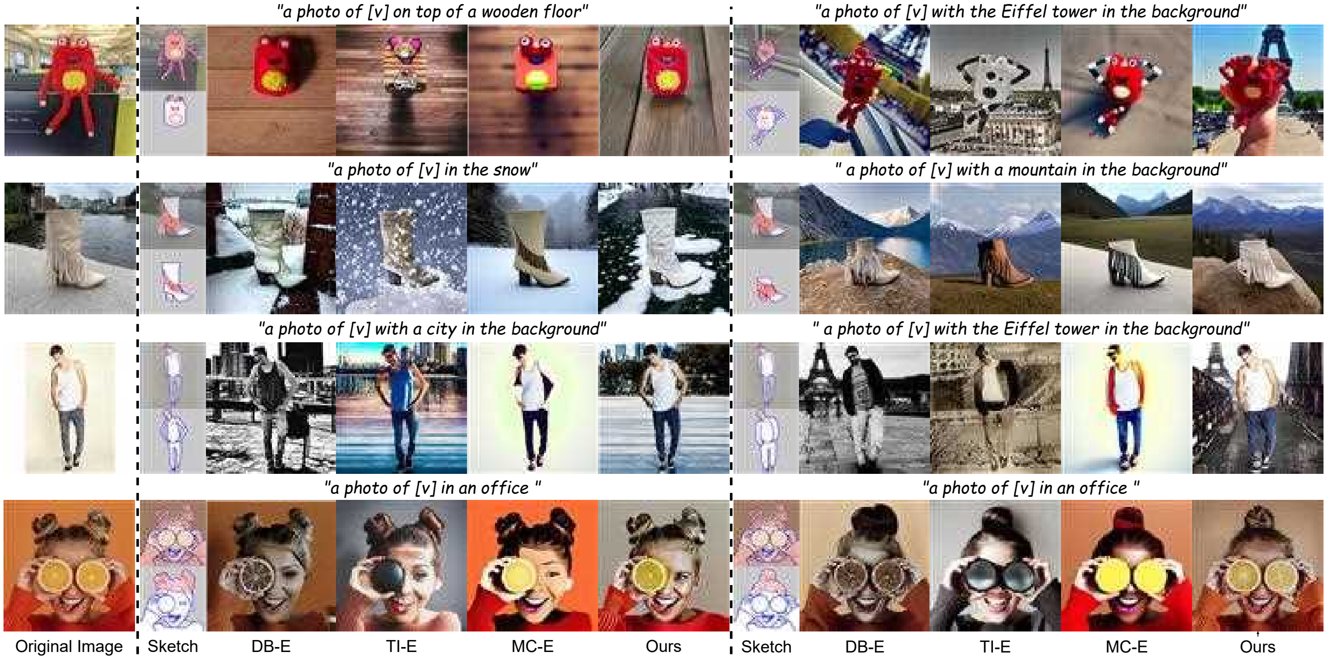
"a photo of [v] on top of a wooden floor"
"a photo of [v] with the Eiffel tower in the background"
"a photo of [v] in the snow"
" a photo of [v] with a mountain in the background"
"a photo of [v] with a city in the background"
" a photo of [v] with the Eiffel tower in the background"
"a photo of [v] in an office "
"a photo of [v] in an office "
Original Image
Sketch
DB-E
TI-E
MC-E
Ours
Sketch
DB-E
TI-E
MC-E
Ours

Figure 4. Comparisons of the results generated by our method and three adapted baselines, given the same text prompt and sketch. In the sketch column, the top one is the annotated sketch corresponding to the original image for training while the bottom one is an edited sketch.

Dataset. Before comparisons, we prepare a dataset of image-sketch pairs covering diverse categories (e.g., toys, human portraits, pets, buildings). We first collect images from the personalization works [21, 31] and the sketch-based work [63]. Next, we invite three normal users without any professional training in drawing to trace the images with separate contour lines S_C and detail lines S_D and then edit several sketches initialized with one of the traced sketches to depict a target object by changing its shape, pose, and/or details. Following the general instruction that S_C depicts a coarse shape while S_D is inside the shape, users decided S_C and S_D by themselves and drew them consistently for training and testing to personalize the sketch concept. Finally, we obtain 35 groups of concept data. Each concept has 1-6 image-sketch pair(s) and 3-5 edited sketches. In total, the dataset contains 102 traced sketches with the corresponding images for training and 159 edited sketches without paired images. Moreover, we employ ten prompt templates for each concept, e.g., "a photo of $[v]$ at the beach", similar to [3]. Thus, the dataset includes 2,610=(102+159)×10 sketch-text pairs (see Supp) for evaluation.

Metrics. We utilize prompt similarity, identity similarity, and perceptual distance as evaluation metrics. Following the prior work [3], the prompt similarity assesses the distance between a text prompt and the corresponding produced images using CLIP model [43]. For computing, the learned token $[v]$ in the prompt is replaced with its class, e.g., "a $[v]$ in the office" is modified to "a woman in the office". The identity similarity measures how the method preserves the object identity of the original image when the context by text or the structure by sketch is changed. We compute the metrics via DINO [9] features as Ruiz et al. [48] did. Additionally, we evaluate the perceptual distance via the LPIPS metric [71] for the reconstruction error regarding appearance and geometry between the ground truth and the generated images given the traced sketches. For identity similarity and perceptual similarity, we adopt the masked version of the results and ground truth to focus on the foreground parts depicted by sketches. Note that we evaluate prompt and identity similarity on all the sketch-text pairs while computing perceptual similarity only on the traced sketches with their paired images.

4.1. Comparison

To our knowledge, we are the first work to extract sketch concepts for image synthesis and editing. To fairly compare our method with the existing personalization techniques, we adapt two methods, TI [21] and DB [48], to fit our proposed task by introducing a pre-trained sketch encoder [36] into their methods when training and testing. Note that we do not optimize the weights of the encoder for the two methods to keep their method intact mostly, and we thus only use a single masked encoder to preserve the pre-trained prior. The two methods receive the dual-sketch representation encoded in one map (i.e., 255 for S_C and 127 for S_D) with a

Table 1. Quantitative comparisons for diverse methods.

Method	Prompt ↑	Identity ↑	Perceptual ↓
DB-E	0.641	0.889	0.182
TI-E	**0.642**	0.867	0.214
MC-E	0.633	0.884	0.16
Single-sketch	0.622	0.908	0.146
w/o $\mathcal{L}_{shape}$	0.639	0.906	0.150
w/o $\mathcal{L}_{reg}$	0.618	0.909	0.142
w/o Masked $\mathcal{F}$	0.620	0.911	0.141
Ours	0.632	**0.912**	**0.134**

mask to have the same inputs as ours. Besides the tuning-based methods, we also compare our method with a tuning-free method, MasaCtrl [8], which can work for sketch-based editing. We directly adopt their released code that integrates the sketch encoder [36] for comparison. All the compared methods are based on SD v1.5 [47]. For simplicity, we refer to the three baselines as TI-E, DB-E, and MC-E.

Figure 4 shows a qualitative comparison between our method and the baselines. Although the editing results by the three baselines are generally faithful to the structure of the edited sketches, they could not preserve the identity or style of the objects/subjects in the original images. Specifically, DB-E can reconstruct the original images with sketches generally (see Supp), but when editing, it often loses the details depicted by the edited sketch and the correspondence between the sketch and target concept defined by the training sketch-image pairs. TI-E cannot recover the original identity in both reconstruction and editing since it merely optimizes high-level text embedding. MC-E tends to drift the result's style from the original one. It is because a) MC adopts a pre-trained sketch encoder with domain bias as discussed in Sec. 1, and thus it could not work well for novel sketch concept; b) this training-free method edits a real image by inverting it to a latent space to leverage the generative prior of a T2I model, but there is a domain gap between the generated images and real images. Our method outperforms the three baselines and maintains the original identity and the sketch-image correspondence defined in the sketch concept.

Table 1 presents the quantitative evaluation results in the three metrics. It demonstrates our method achieves the best identity preservation (identity similarity) and reconstruction quality (perceptual distance). However, our method sacrifices slightly the prompt similarity since we focus on the reconstruction of the foreground object with $\mathcal{L}_{shape}$ (see the ablation study without $\mathcal{L}_{shape}$). Such sacrifice is acceptable to trade off the concept re-creation and sketch faithfulness, as shown in Figures 4 and 5.

Perceptive User Study. We performed a perceptive user study including two evaluations: text editability study and sketch editability study. We first prepared a subset (30 randomly picked concepts, 15 for prompt similarity, 15 for sketch faithfulness) of our collected dataset. For text editability, we produced the results by the three baselines and our method given a traced sketch and a prompt randomly picked from one concept. A participant was given a reference image, a prompt (e.g., "a photo of the boots in the reference image in the snow"), and the four generated results in random order. We asked the participants to rate "How the result is consistent with the prompt" on a Likert scale of 1–5 (the higher, the better). For sketch editability, we presented each participant with a reference image with the traced sketch, an edited sketch, and four results (in random order) and required them to rate "How the result is faithful to the edited sketch and consistent with the reference identity". From 40 participants, we received 600 responses for each method in each evaluation. As shown in Figure 5, the user study reflects the superiority of our method to the baselines in both evaluations.

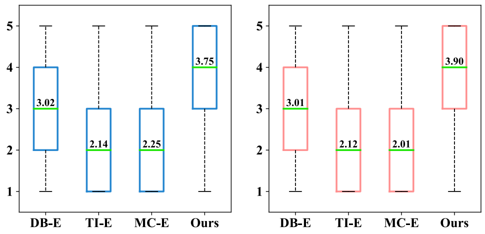

(a) Text Editability (b) Sketch Editability

Figure 5. Box plots of the ratings in the perceptive user study. Each value above the median line is the average rate for each method. The higher, the better.

4.2. Ablation Study

We ablated one of the key settings of our method to validate their effectiveness, including 1) w/ single-sketch representation; 2) w/o shape loss $\mathcal{L}_{shape}$; 3) w/o regularization loss $\mathcal{L}_{reg}$; 4) w/o masked encoder $\mathcal{F}$. As shown in Figure 6, using the single-sketch representation could not provide sufficient constraints on shapes (e.g., the castle and bear toy) and details (e.g., the woman's clothes), damaging the identity preservation. Removing $\mathcal{L}_{shape}$ would produce redundant parts and weaken the concept reconstruction. Without $\mathcal{L}_{reg}$, the method would overfit to the original shape and worsen the sketch editability (see Figures 6 & 7). Additionally, removing either $\mathcal{L}_{reg}$ or the masked $\mathcal{F}$ would affect a lot the text editability for background, shown as Figure 7. It is because $\mathcal{L}_{reg}$ can prevent the global embedding from enlarging significantly to outweigh the background token, while the masked $\mathcal{F}$ can filter out the local background features from the empty region of the sketch. The quantitative results in Table 1 further confirm the above conclusions.

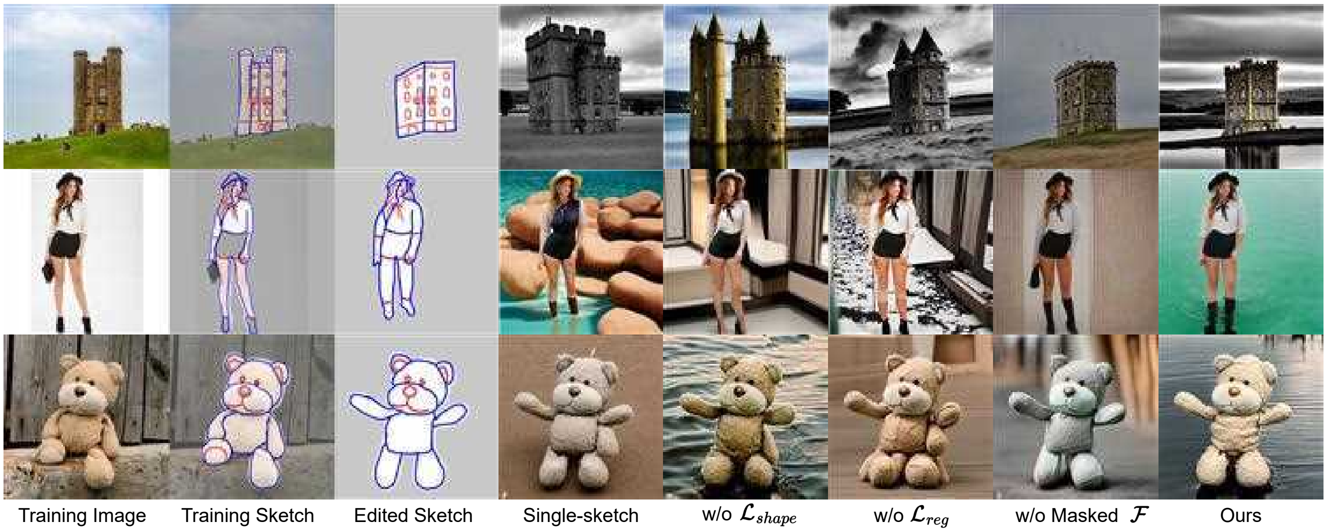

Figure 6. Comparisons of our results and those by the ablated variants, given the text prompt "A photo of $[v]$ floating on top of water".

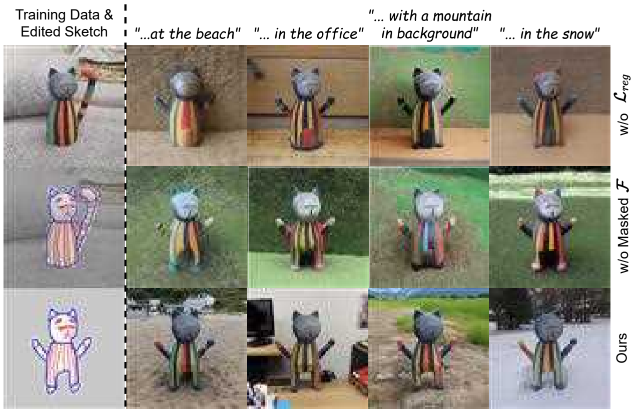

Figure 7. Comparisons of the results by ours and the ablated variants using one edited sketch and diverse prompts indicating different contexts. The prefix of the prompt is *"A photo of* $[v]$ *..."*.

4.3. Applications

We implemented four applications enabled by our method: local editing, concept transfer, multi-concept generation, and text-based style variation. We showcase the applications in Figure 8 to demonstrate the effectiveness and versatility of *CustomSketching*. Please refer to Supp for the implementation details for each application.

Local Editing. After extracting a sketch concept from reference image(s), we can perform local editing on the original images, including modification, addition, and removal. To keep the unedited region intact, we incorporate our method with an off-the-shelf local editing method by Avrahami et al. [4]. Users can edit the training sketch and provide a mask for the region they want to manipulate for fine-grained local editing (see Figure 8 (a)).

Concept Transfer. Given different concepts separately learned from the corresponding sketch-image pairs, our method can transfer between the concepts ($[S_i]$=$\{[v_i], \mathcal{F}_i\}$) with similar semantics via sketches. Figure 8 (b) shows an example of hairstyle transfer. Note that we also resort to [4] for local transfer.

Multi-concept Generation. For multi-concept generation, prior works [3, 31] need to fine-tune the model on all the concepts desired in generation jointly. Unlike these works, which optimize the entire denoising network, we only optimize $[v]$ and $\mathcal{F}$ for one concept. This lightweight setting enables our method to achieve plug-and-play multi-concept generation by separately learning each concept and then combining them freely without extra optimization. Figure 8 (c) presents two cases of the combinations among three extracted sketch concepts ($[S_1]$, $[S_2]$, $[S_3]$).

Text-based Style Variation. Our method decouples global semantics and local features of a reference image to a textual token $[v]$ and a sketch encoder $\mathcal{F}$. Thus, our method can be used to produce diverse style variations of the target object while preserving its geometry (shape and details), as shown in Figure 8 (d). To this end, our method takes as input the sketch (regarded as an intermediate representation of object geometry) and a style prompt without $[v]$ (e.g., "a crayon drawing") to control the target style. We compare our method with PnP [54], a text-based image-to-image translation method, by feeding a masked image with the style prompt to this method. Thanks to the given sketch, our method can better disentangle the geometry and style, thus offering more user controllability and flexibility via sketching.

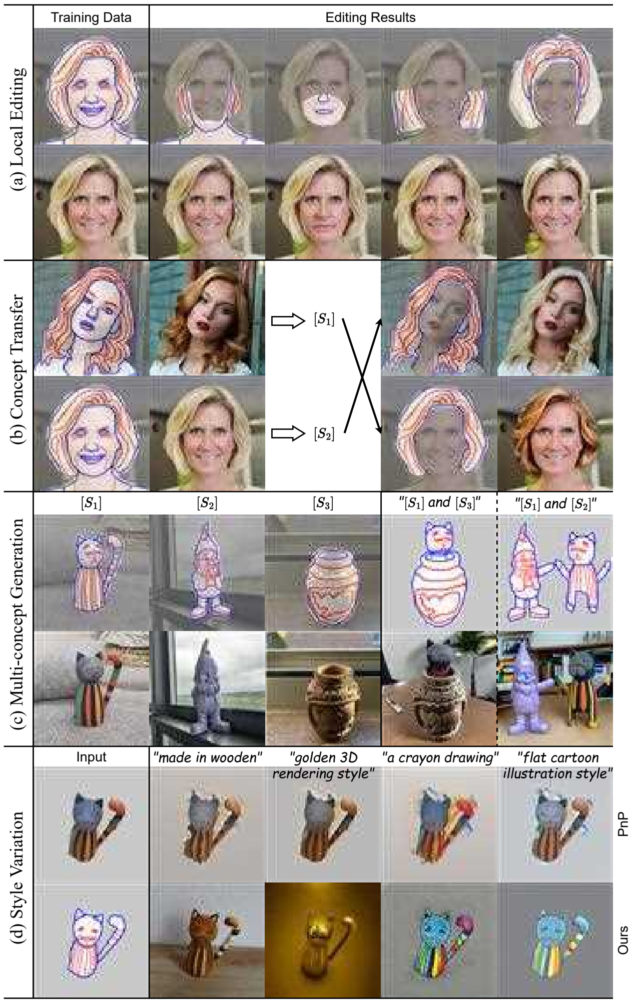

Figure 8. Four applications enabled by our *CustomSketching*. For (c), the template of the prompt is *"A photo of* $[S_i]$ *in an office"*.

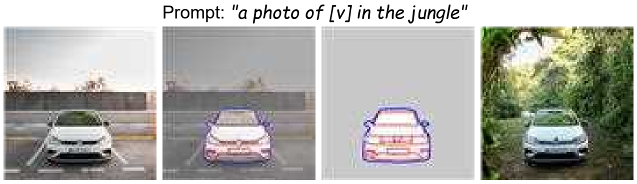

Figure 9. One failure case of our method. Our method could not change the car's tiny details by sketching thin strokes.

5. Conclusion and Discussion

We proposed *CustomSketching*, a novel approach to extract sketch concepts for sketch-based image synthesis and editing based on a large T2I model. This method decouples reference image(s) into global semantics in a textual token and local features in two sketch encoders. We presented a dual-sketch representation to differentiate the shape and details of one concept. In this way, our method empowers users with high controllability in local and fine-grained image editing. Extensive experiments and several applications have shown the effectiveness and superiority of our proposed method to the alternative solutions. We will release the dataset and code to the research community.

While our method improves the controllability and flexibility of the personalization task, it has several limitations. First, inherited from latent diffusion models, our method processes images in a low-resolution latent space (64×64). It thus struggles to control an object's tiny shape and details by sketching thin strokes. As shown in Figure 9, the car's details could not be changed following the edited sketch. Another limitation is the learning efficiency. Currently, our method requires almost 30 mins to learn one concept for two-stage optimization. In the future, we may use fast personalization techniques [23, 28] to address this issue.

References

[1] Rameen Abdal, Peihao Zhu, John Femiani, Niloy Mitra, and Peter Wonka. Clip2stylegan: Unsupervised extraction of stylegan edit directions. In *ACM SIGGRAPH 2022 conference proceedings*, pages 1–9, 2022. 3

[2] Omri Avrahami, Dani Lischinski, and Ohad Fried. Blended diffusion for text-driven editing of natural images. In *CVPR*, pages 18208–18218, 2022. 3

[3] Omri Avrahami, Kfir Aberman, Ohad Fried, Daniel Cohen-Or, and Dani Lischinski. Break-a-scene: Extracting multiple concepts from a single image. *arXiv preprint arXiv:2305.16311*, 2023. 2, 3, 4, 5, 6, 8, 13

[4] Omri Avrahami, Ohad Fried, and Dani Lischinski. Blended latent diffusion. *ACM TOG*, 42(4):1–11, 2023. 3, 8, 15

[5] David Bau, Alex Andonian, Audrey Cui, YeonHwan Park, Ali Jahanian, Aude Oliva, and Antonio Torralba. Paint by word. *arXiv preprint arXiv:2103.10951*, 2021. 3

[6] Andrew Brock, Jeff Donahue, and Karen Simonyan. Large scale gan training for high fidelity natural image synthesis. In *ICLR*, 2018. 3

[7] Tim Brooks, Aleksander Holynski, and Alexei A Efros. Instructpix2pix: Learning to follow image editing instructions. In *CVPR*, pages 18392–18402, 2023. 3

[8] Mingdeng Cao, Xintao Wang, Zhongang Qi, Ying Shan, Xiaohu Qie, and Yinqiang Zheng. Masactrl: Tuning-free mutual self-attention control for consistent image synthesis and editing. In *ICCV*, pages 22560–22570, 2023. 3, 7, 14

[9] Mathilde Caron, Hugo Touvron, Ishan Misra, Hervé Jégou, Julien Mairal, Piotr Bojanowski, and Armand Joulin. Emerging properties in self-supervised vision transformers. In *ICCV*, pages 9650–9660, 2021. 6

[10] Hila Chefer, Yuval Alaluf, Yael Vinker, Lior Wolf, and Daniel Cohen-Or. Attend-and-excite: Attention-based semantic guidance for text-to-image diffusion models. *ACM TOG*, 42(4):1–10, 2023. 5

[11] Shu-Yu Chen, Wanchao Su, Lin Gao, Shihong Xia, and Hongbo Fu. Deepfacedrawing: Deep generation of face images from sketches. *ACM TOG*, 39(4):72–1, 2020. 3

[12] Shu-Yu Chen, Feng-Lin Liu, Yu-Kun Lai, Paul L Rosin, Chunpeng Li, Hongbo Fu, and Lin Gao. Deepfaceediting: deep face generation and editing with disentangled geometry and appearance control. *ACM TOG*, 40(4):1–15, 2021. 3

[13] Wengling Chen and James Hays. Sketchygan: Towards diverse and realistic sketch to image synthesis. In *CVPR*, pages 9416–9425, 2018. 3

[14] Wenhu Chen, Hexiang Hu, Yandong Li, Nataniel Rui, Xuhui Jia, Ming-Wei Chang, and William W Cohen. Subject-driven text-to-image generation via apprenticeship learning. 2023. 3

[15] Xi Chen, Lianghua Huang, Yu Liu, Yujun Shen, Deli Zhao, and Hengshuang Zhao. Anydoor: Zero-shot object-level image customization. *arXiv preprint arXiv:2307.09481*, 2023. 2, 3

[16] Shin-I Cheng, Yu-Jie Chen, Wei-Chen Chiu, Hung-Yu Tseng, and Hsin-Ying Lee. Adaptively-realistic image generation from stroke and sketch with diffusion model. In *Proceedings of the IEEE/CVF Winter Conference on Applications of Computer Vision*, pages 4054–4062, 2023. 3

[17] Kyunghyun Cho, Bart Van Merriënboer, Dzmitry Bahdanau, and Yoshua Bengio. On the properties of neural machine translation: Encoder-decoder approaches. *arXiv preprint arXiv:1409.1259*, 2014. 3

[18] Guillaume Couairon, Jakob Verbeek, Holger Schwenk, and Matthieu Cord. Diffedit: Diffusion-based semantic image editing with mask guidance. In *ICLR*, 2022. 3

[19] Katherine Crowson, Stella Biderman, Daniel Kornis, Dashiell Stander, Eric Hallahan, Louis Castricato, and Edward Raff. Vqgan-clip: Open domain image generation and editing with natural language guidance. In *ECCV*, pages 88–105. Springer, 2022. 3

[20] Prafulla Dhariwal and Alexander Nichol. Diffusion models beat gans on image synthesis. *Advances in neural information processing systems*, 34:8780–8794, 2021. 3

[21] Rinon Gal, Yuval Alaluf, Yuval Atzmon, Or Patashnik, Amit Haim Bermano, Gal Chechik, and Daniel Cohen-or. An image is worth one word: Personalizing text-to-image generation using textual inversion. In *ICLR*, 2022. 2, 3, 4, 6, 13

[22] Rinon Gal, Or Patashnik, Haggai Maron, Amit H Bermano, Gal Chechik, and Daniel Cohen-Or. Stylegan-nada: Clip-guided domain adaptation of image generators. *ACM TOG*, 41(4):1–13, 2022. 3

[23] Rinon Gal, Moab Arar, Yuval Atzmon, Amit H Bermano, Gal Chechik, and Daniel Cohen-Or. Encoder-based domain tuning for fast personalization of text-to-image models. *ACM TOG*, 42(4):1–13, 2023. 3, 9

[24] Ian Goodfellow, Jean Pouget-Abadie, Mehdi Mirza, Bing Xu, David Warde-Farley, Sherjil Ozair, Aaron Courville, and Yoshua Bengio. Generative adversarial nets. *Advances in neural information processing systems*, 27, 2014. 3

[25] Amir Hertz, Ron Mokady, Jay Tenenbaum, Kfir Aberman, Yael Pritch, and Daniel Cohen-or. Prompt-to-prompt image editing with cross-attention control. In *ICLR*, 2022. 3, 5, 13

[26] Jonathan Ho, Ajay Jain, and Pieter Abbeel. Denoising diffusion probabilistic models. *NeurIPS*, 33:6840–6851, 2020. 3

[27] Sepp Hochreiter and Jürgen Schmidhuber. Long short-term memory. *Neural computation*, 9(8):1735–1780, 1997. 3

[28] Xuhui Jia, Yang Zhao, Kelvin CK Chan, Yandong Li, Han Zhang, Boqing Gong, Tingbo Hou, Huisheng Wang, and Yu-Chuan Su. Taming encoder for zero fine-tuning image customization with text-to-image diffusion models. *arXiv preprint arXiv:2304.02642*, 2023. 3, 9

[29] Tero Karras, Samuli Laine, and Timo Aila. A style-based generator architecture for generative adversarial networks. In *CVPR*, pages 4401–4410, 2019. 3

[30] Bahjat Kawar, Shiran Zada, Oran Lang, Omer Tov, Huiwen Chang, Tali Dekel, Inbar Mosseri, and Michal Irani. Imagic: Text-based real image editing with diffusion models. In *CVPR*, pages 6007–6017, 2023. 3

[31] Nupur Kumari, Bingliang Zhang, Richard Zhang, Eli Shechtman, and Jun-Yan Zhu. Multi-concept customization of text-to-image diffusion. In *CVPR*, pages 1931–1941, 2023. 2, 3, 6, 8

[32] Feng-Lin Liu, Shu-Yu Chen, Yukun Lai, Chunpeng Li, Yue-Ren Jiang, Hongbo Fu, and Lin Gao. Deepfacevideoediting: sketch-based deep editing of face videos. *ACM TOG*, 41(4): 167, 2022. 3

[33] Yifang Men, Yiming Mao, Yuning Jiang, Wei-Ying Ma, and Zhouhui Lian. Controllable person image synthesis with attribute-decomposed gan. In *CVPR*, pages 5084–5093, 2020. 3

[34] Ron Mokady, Omer Tov, Michal Yarom, Oran Lang, Inbar Mosseri, Tali Dekel, Daniel Cohen-Or, and Michal Irani. Self-distilled stylegan: Towards generation from internet photos. In *ACM SIGGRAPH 2022 Conference Proceedings*, pages 1–9, 2022. 3

[35] Ron Mokady, Amir Hertz, Kfir Aberman, Yael Pritch, and Daniel Cohen-Or. Null-text inversion for editing real images using guided diffusion models. In *CVPR*, pages 6038–6047, 2023. 3

[36] Chong Mou, Xintao Wang, Liangbin Xie, Jian Zhang, Zhongang Qi, Ying Shan, and Xiaohu Qie. T2i-adapter: Learning adapters to dig out more controllable ability for text-to-image diffusion models. *arXiv preprint arXiv:2302.08453*, 2023. 2, 3, 4, 5, 6, 7, 13

[37] Alexander Quinn Nichol, Prafulla Dhariwal, Aditya Ramesh, Pranav Shyam, Pamela Mishkin, Bob Mcgrew, Ilya Sutskever, and Mark Chen. Glide: Towards photorealistic image generation and editing with text-guided diffusion models. In *International Conference on Machine Learning*, pages 16784–16804. PMLR, 2022. 3

[38] Yotam Nitzan, Kfir Aberman, Qiurui He, Orly Liba, Michal Yarom, Yossi Gandelsman, Inbar Mosseri, Yael Pritch, and Daniel Cohen-Or. Mystyle: A personalized generative prior. *ACM TOG*, 41(6):1–10, 2022. 3

[39] Or Patashnik, Zongze Wu, Eli Shechtman, Daniel Cohen-Or, and Dani Lischinski. Styleclip: Text-driven manipulation of stylegan imagery. In *ICCV*, pages 2085–2094, 2021. 3

[40] Or Patashnik, Daniel Garibi, Idan Azuri, Hadar Averbuch-Elor, and Daniel Cohen-Or. Localizing object-level shape variations with text-to-image diffusion models. 2023. 3

[41] Yichen Peng, Chunqi Zhao, Haoran Xie, Tsukasa Fukusato, and Kazunori Miyata. Difffacesketch: High-fidelity face image synthesis with sketch-guided latent diffusion model. *arXiv preprint arXiv:2302.06908*, 2023. 3

[42] Tiziano Portenier, Qiyang Hu, Attila Szabó, Siavash Arjomand Bigdeli, Paolo Favaro, and Matthias Zwicker. Faceshop: deep sketch-based face image editing. *ACM Transactions on Graphics (TOG)*, 37(4):1–13, 2018. 3

[43] Alec Radford, Jong Wook Kim, Chris Hallacy, Aditya Ramesh, Gabriel Goh, Sandhini Agarwal, Girish Sastry, Amanda Askell, Pamela Mishkin, Jack Clark, et al. Learning transferable visual models from natural language supervision. In *International conference on machine learning*, pages 8748–8763. PMLR, 2021. 3, 6

[44] Aditya Ramesh, Mikhail Pavlov, Gabriel Goh, Scott Gray, Chelsea Voss, Alec Radford, Mark Chen, and Ilya Sutskever. Zero-shot text-to-image generation. In *ICML*, pages 8821–8831. PMLR, 2021. 2, 3

[45] Scott Reed, Zeynep Akata, Xinchen Yan, Lajanugen Logeswaran, Bernt Schiele, and Honglak Lee. Generative adversarial text to image synthesis. In *International conference on machine learning*, pages 1060–1069. PMLR, 2016. 3

[46] Elad Richardson, Yuval Alaluf, Or Patashnik, Yotam Nitzan, Yaniv Azar, Stav Shapiro, and Daniel Cohen-Or. Encoding in style: a stylegan encoder for image-to-image translation. In *CVPR*, pages 2287–2296, 2021. 3

[47] Robin Rombach, Andreas Blattmann, Dominik Lorenz, Patrick Esser, and Björn Ommer. High-resolution image synthesis with latent diffusion models. In *CVPR*, pages 10684–10695, 2022. 2, 3, 7, 13

[48] Nataniel Ruiz, Yuanzhen Li, Varun Jampani, Yael Pritch, Michael Rubinstein, and Kfir Aberman. Dreambooth: Fine tuning text-to-image diffusion models for subject-driven generation. In *CVPR*, pages 22500–22510, 2023. 2, 3, 6, 13

[49] Chitwan Saharia, William Chan, Saurabh Saxena, Lala Li, Jay Whang, Emily L Denton, Kamyar Ghasemipour, Raphael Gontijo Lopes, Burcu Karagol Ayan, Tim Salimans, et al. Photorealistic text-to-image diffusion models with deep language understanding. *NIPS*, 35:36479–36494, 2022. 2

[50] Patsorn Sangkloy, Jingwan Lu, Chen Fang, Fisher Yu, and James Hays. Scribbler: Controlling deep image synthesis with sketch and color. In *CVPR*, pages 5400–5409, 2017. 3

[51] Jing Shi, Wei Xiong, Zhe Lin, and Hyun Joon Jung. Instantbooth: Personalized text-to-image generation without test-time finetuning. *arXiv preprint arXiv:2304.03411*, 2023. 3

[52] Jiaming Song, Chenlin Meng, and Stefano Ermon. Denoising diffusion implicit models. In *ICLR*, 2020. 3

[53] Yang Song and Stefano Ermon. Generative modeling by estimating gradients of the data distribution. *NeurIPS*, 32, 2019. 3

[54] Narek Tumanyan, Michal Geyer, Shai Bagon, and Tali Dekel. Plug-and-play diffusion features for text-driven image-to-image translation. In *CVPR*, pages 1921–1930, 2023. 8, 16, 18

[55] Dani Valevski, Matan Kalman, Eyal Molad, Eyal Segalis, Yossi Matias, and Yaniv Leviathan. Unitune: Text-driven image editing by fine tuning a diffusion model on a single image. *ACM TOG*, 42(4):1–10, 2023. 3

[56] Ashish Vaswani, Noam Shazeer, Niki Parmar, Jakob Uszkoreit, Llion Jones, Aidan N Gomez, Łukasz Kaiser, and Illia Polosukhin. Attention is all you need. *NIPS*, 30, 2017. 3

[57] Yael Vinker, Eliahu Horwitz, Nir Zabari, and Yedid Hoshen. Image shape manipulation from a single augmented training sample. In *ICCV*, pages 13769–13778, 2021. 3

[58] Andrey Voynov, Kfir Aberman, and Daniel Cohen-Or. Sketch-guided text-to-image diffusion models. In *ACM SIGGRAPH 2023 Conference Proceedings*, pages 1–11, 2023. 3

[59] Qiang Wang, Di Kong, Fengyin Lin, and Yonggang Qi. Diffsketching: Sketch control image synthesis with diffusion models. 2023. 3

[60] Su Wang, Chitwan Saharia, Ceslee Montgomery, Jordi Pont-Tuset, Shai Noy, Stefano Pellegrini, Yasumasa Onoe, Sarah Laszlo, David J Fleet, Radu Soricut, et al. Imagen editor and editbench: Advancing and evaluating text-guided image inpainting. In *CVPR*, pages 18359–18369, 2023. 3

[61] Yuxiang Wei, Yabo Zhang, Zhilong Ji, Jinfeng Bai, Lei Zhang, and Wangmeng Zuo. Elite: Encoding visual concepts into textual embeddings for customized text-to-image generation. 2023. 3

[62] Weihao Xia, Yujiu Yang, Jing-Hao Xue, and Baoyuan Wu. Tedigan: Text-guided diverse face image generation and manipulation. In *CVPR*, pages 2256–2265, 2021. 3

[63] Chufeng Xiao, Deng Yu, Xiaoguang Han, Youyi Zheng, and Hongbo Fu. Sketchhairsalon: deep sketch-based hair image synthesis. *ACM TOG*, 40(6):1–16, 2021. 3, 6

[64] Tao Xu, Pengchuan Zhang, Qiuyuan Huang, Han Zhang, Zhe Gan, Xiaolei Huang, and Xiaodong He. Attngan: Fine-grained text to image generation with attentional generative adversarial networks. In *CVPR*, pages 1316–1324, 2018. 3

[65] Yiwen Xu, Ruoyu Guo, Maurice Pagnucco, and Yang Song. Draw2edit: Mask-free sketch-guided image manipulation. In *Proceedings of the 31st ACM International Conference on Multimedia*, pages 7205–7215, 2023. 3

[66] Yu Zeng, Zhe Lin, and Vishal M Patel. Sketchedit: Mask-free local image manipulation with partial sketches. In *Proceedings of the IEEE/CVF Conference on Computer Vision and Pattern Recognition*, pages 5951–5961, 2022. 3

[67] Han Zhang, Tao Xu, Hongsheng Li, Shaoting Zhang, Xiaogang Wang, Xiaolei Huang, and Dimitris N Metaxas. Stackgan: Text to photo-realistic image synthesis with stacked generative adversarial networks. In *ICCV*, pages 5907–5915, 2017. 3

[68] Han Zhang, Tao Xu, Hongsheng Li, Shaoting Zhang, Xiaogang Wang, Xiaolei Huang, and Dimitris N Metaxas. Stackgan++: Realistic image synthesis with stacked generative adversarial networks. *IEEE TPAMI*, 41(8):1947–1962, 2018.

[69] Han Zhang, Jing Yu Koh, Jason Baldridge, Honglak Lee, and Yinfei Yang. Cross-modal contrastive learning for text-to-image generation. In *CVPR*, pages 833–842, 2021. 3

[70] Lvmin Zhang, Anyi Rao, and Maneesh Agrawala. Adding conditional control to text-to-image diffusion models. In *ICCV*, pages 3836–3847, 2023. 2, 3, 4, 14

[71] Richard Zhang, Phillip Isola, Alexei A Efros, Eli Shechtman, and Oliver Wang. The unreasonable effectiveness of deep features as a perceptual metric. In *CVPR*, pages 586–595, 2018. 6

[72] Yuechen Zhang, Jinbo Xing, Eric Lo, and Jiaya Jia. Real-world image variation by aligning diffusion inversion chain. *NIPS*, 2023. 14

[73] Changqing Zou, Haoran Mo, Chengying Gao, Ruofei Du, and Hongbo Fu. Language-based colorization of scene sketches. *ACM TOG*, 38(6):1–16, 2019. 3

CustomSketching: Sketch Concept Extraction for Sketch-based Image Synthesis and Editing

Supplementary Material

6. Dataset

Figure 19 shows a thumbnail of our created dataset, covering diverse object categories. For each object regarded as one concept, we invited three normal users without any professional training in drawing to trace separate contour lines S_C and details lines S_D over the reference images. One training sketch traced over an image generally cost 30s-2min for an amateur, while a testing one cost less than 1min. The sketch-image pairs are with purple borders in Figure 19. Note that each concept has 1-6 image-sketch pair(s) for training, where the concepts of human portrait and clothing only have a single pair. Then, the users were asked to create 3-5 edited dual sketches (with yellow borders in Figure 19) initialized from one of the traced sketches or drawn from scratch. In this way, we created the concepts with different fine-grained attributes (shape, pose, details) from the reference images, represented by the edited sketches. For each traced or edited sketch, we used a polygon filling method (implemented via OpenCV v3) to automatically generate a foreground mask following S_C. The automatically generated masks were generally accurate but the annotators were allowed to manually refine the masks if necessary. Finally, we obtained 35 groups of concept data, with 102 traced sketches with paired images, 159 edited sketches, as well as foreground masks corresponding to both sketches. Similar to [3], we set up ten prompt templates with the learned textual token $[v]$ as follows:

- *"A photo of* $[v]$ *at the beach"*
- *"A photo of* $[v]$ *in the jungle"*
- *"A photo of* $[v]$ *in the snow"*
- *"A photo of* $[v]$ *in the street"*
- *"A photo of* $[v]$ *on top of a wooden floor"*
- *"A photo of* $[v]$ *with a city in the background"*
- *"A photo of* $[v]$ *with a mountain in the background"*
- *"A photo of* $[v]$ *with the Eiffel tower in the background"*
- *"A photo of* $[v]$ *floating on top of water"*
- *"A photo of* $[v]$ *in an office"*

Therefore, we have 2,610 = (102+159)×10 sketch-text pairs for evaluation.

7. Implementation Details

Our method and all the compared baselines were based on Stable Diffusion v1.5 [47]. A training image and its corresponding sketch were both resized to 512×512. The sketch features extracted from a sketch encoder $\mathcal{F}$ were injected into four layers of the encoder of the denoising U-net, with resolutions of 64, 32, 16, and 8, following the settings of [36]. For the optimization of Stage I, we only fine-tuned a newly added textual token $[v]$ with a learning rate of $5e^{-4}$. The token was initialized using the class name of the target concept, e.g., "toy" for the toy object. The sketch encoder for Stage I is a pre-trained model (*t2iadapter_sketch_sd15v2*) from [36] with frozen weights during optimization. For Stage II, we jointly optimized the token $[v]$ and two sketch encoders with a small learning rate of $2e^{-6}$, similar to [3]. The weights of the two sketch encoders were initialized with those of the pre-trained one [36] used in Stage I. During training, a text prompt as input was randomly selected from the list of text templates in [21], while during testing, the prompt was picked from our created dataset. Empirically, we trained each stage in our experiment for 400 steps (batch size=16) using the Adam solver via the PyTorch framework. We randomly augmented (with the probability of 0.5) the training data by translating each sketch-image pair in the range of [-0.2,0.2], rotating it in the range of [-45°,45°], and horizontal flip. We trained and tested our method *CustomSketching* on a PC with Intel i9-13900K, 128GB RAM, and a single NVIDIA GeForce RTX 4090. The two-stage optimization took around 30 mins, while one pass inference (DDPM sampling with 50 steps) cost around 3s.

We used cross-attention maps in each layer of the denoising U-Net to compute shape loss $\mathcal{L}_{shape}$. Following Hertz et al. [25], we combined and averaged all the cross-attention maps $A_\theta(z_t, v)$ of the token $[v]$. The different layers of the attention maps with diverse resolutions were resized to 16×16 for computation.

8. Experiments

Comparisons with SOTAs. In the main text, we adapted DB [48] and TI [21] with a pre-trained sketch encoder [36] to fit the task of sketch concept extraction, refer to DB-E and TI-E. Since DB learned a novel concept by binding a unique identifier (e.g., *"sks"*) with a specific subject in a text prompt, we provided a text prompt like *"a photo of a sks toy"* for the toy category for training and testing. Note that the weights of the sketch encoder in DB-E and TI-E were frozen to keep the two methods intact mostly. In the Supp, we further adapted DB and TI with two learnable sketch encoders fed with the dual-sketch representation as ours did, respectively referring to DB-FE and TI-FE. Considering vanilla DB might have enough capacity to learn a

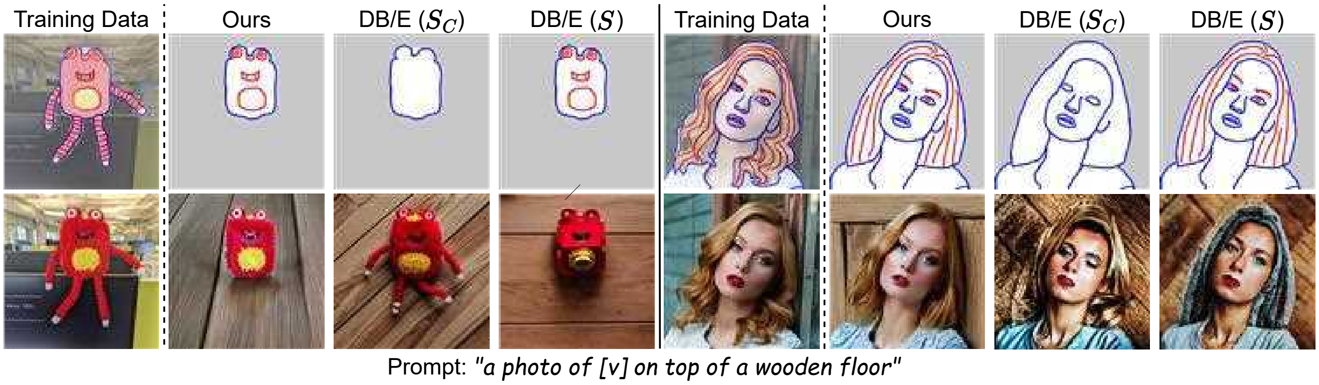

Figure 10. Qualitative comparison between ours and vanilla DB with a pre-trained sketch T2I-adapter (DB/E). The results show DB/E fails in correctly reconstruction and editing the reference image.

concept without sketch condition, we also separately compared our method with vanilla DB (denoted as DB/E), i.e., training vanilla DB for one concept and testing it with a pre-trained T2I-adapter (without fine-tuning). Fig. 10 shows two evaluation results on the sketch with only S_C (DB/E (S_C)) and the sketch with both types (DB/E (S)). It can be easily found that DB/E fails to correctly reconstruct the concept without sufficient sketch constraint and edit the concept using detail strokes due to the domain gap existing in the pre-trained sketch encoder. The above tuning-based methods (DB/E, DB-FE, DB-E, TI-FE, TI-E) had the same training parameters and augmentation tricks as ours.

For tuning-free methods, we compared our method with MS-E [8] in the main text, but we found it often drifted the original style of the reference images due to the gap between the generated images and real images. A follow-up work, RIVAL [72], was proposed to alleviate such a gap. RIVAL employed a pre-trained ControlNet [70] to enable sketch-based editing for real images. We also compared our method with the sketch-based version of RIVAL (denoted as RIVAL-E) by directly using their released code. The tuning-based methods consist of an inversion step and an inference step. For the inversion step, we provided a reference image with the traced sketch and a text prompt (e.g., *"a photo of a toy"* for the toy category), while for the inference step, we provided an edited sketch with a target prompt (e.g., *"a photo of a toy in the snow"*). Note that for the tuning-free methods, we used the single-sketch representation for the sketch input to make the method compatible with the prior of the pre-trained sketch encoder. We used the same random seed (seed=42) for our method and all the above baselines during inference.

Figure 20 shows more qualitative comparisons. It demonstrates that our method performs better in sketch- and text-based editing while preserving the annotated object's original identity compared to all the baselines. DB-FE, TI-FE, and RIVAL-E can improve the reconstruction quality a little in appearance and geometry, respectively compared to DB-E, TI-E, and MS-E. However, the three methods still could not achieve satisfactory editing results. The quantitative results could also reflect such a tendency (see Table 2).

Table 2. Quantitative comparisons for diverse methods.

Method	Prompt ↑	Identity ↑	Perceptual ↓
DB/E (S_C)	**0.647**	0.868	0.202
DB/E (S)	**0.647**	0.870	0.196
DB-FE	0.642	0.879	0.192
DB-E	0.641	0.889	0.182
TI-FE	0.634	0.906	0.165
TI-E	0.642	0.867	0.214
RIVAL-E	0.627	0.899	0.151
MS-E	0.633	0.884	0.16
Single-encoder	0.623	0.910	0.142
Single-sketch	0.622	0.908	0.146
w/o $\mathcal{L}_{shape}$	0.639	0.906	0.150
w/o $\mathcal{L}_{reg}$	0.618	0.909	0.142
w/o Masked $\mathcal{F}$	0.620	0.911	0.141
w/o Stage I	0.632	0.904	0.164
Ours	0.632	**0.912**	**0.134**

Ablation Study. Figure 21 shows more results for comparisons between our method and the ablated ones mentioned in the main text. We show two more ablated variants here: 1) adopting a single encoder in Stage II with the dual-sketch representation, i.e., merging S_C and S_D into one sketch map as input; 2) w/o Stage I, i.e., only jointly optimizing a newly added token and the two sketch encoders. As shown in Figure 21 and Table 2, the single-encoder setting could not effectively differentiate shape and details, thus causing worse sketch faithfulness and identity preservation than ours. Removing Stage I results in unsatisfactory

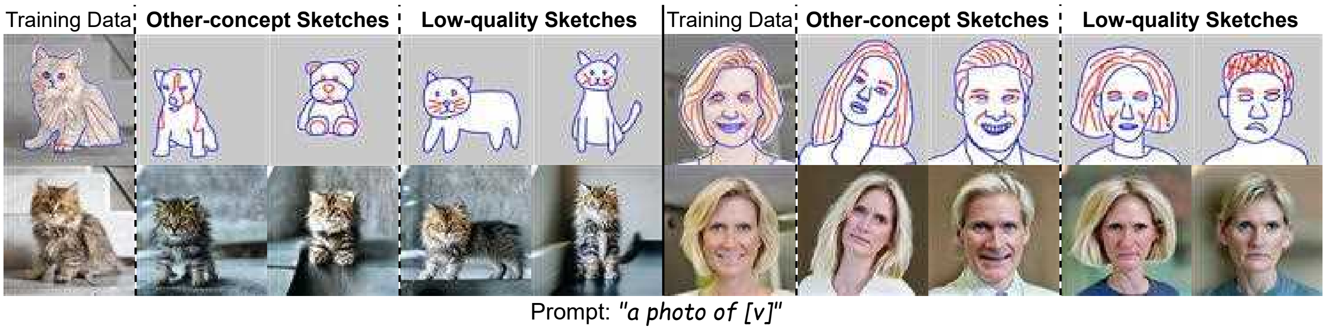

Figure 11. Diverse results given different sketches with the same text prompt and random seed.

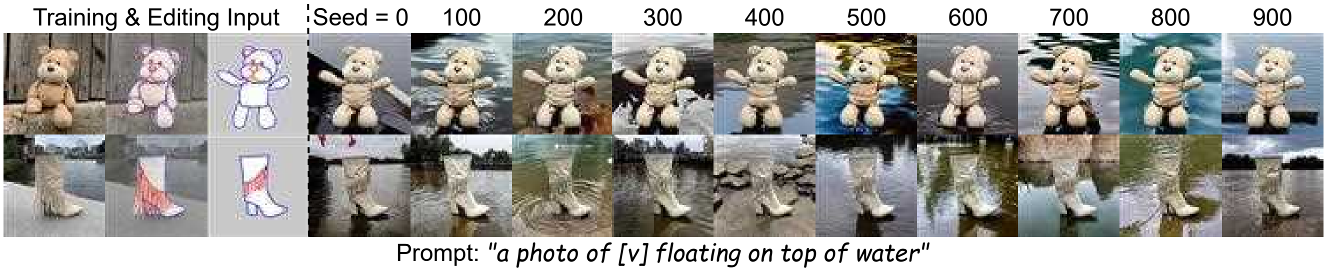

Figure 12. Multiple random seeds with the same text and sketch for sampling diverse results.

reconstruction since the setting would mislead the optimization in disentangling the global semantics into $[v]$ and local features into $\mathcal{F}$. Table 2 also confirms such a conclusion (see the identity similarity and perceptual distance).

Robustness Evaluation. We show the robustness of our method from two aspects: **1) Inputing sketches different from the training samples.** Our method can effectively avoid the T2I-adapter overfitting on given sketches thanks to our optimization settings, thus tolerating sketches different from the training data. This is why our method can be successfully applied to concept transfer (see Main-text Figure 8 & Figure 16). Figure 11 shows more results given two cases of different sketches, i.e., sketches from other concepts and low-quality sketches. **2) Multiple Random Seeds.** We show diverse results given multiple random seeds with the same text and sketch (Figure 12). Since the foreground object is conditioned on the text and sketch, denoising with different seeds mainly varies the background generation, and our method can perform stable to make sure the foreground object is always faithful to the sketch given diverse seeds.

9. Applications

We implemented four applications enabled by our *CustomSketching*. Below, we show more results and the implementation details.

Local Editing. Incorporating [4], our method can be applied to local image editing, which allows users to edit a local region of a given real image via sketching while keeping the unedited region intact. Figure 14 shows the pipeline of such an application. After extracting a novel concept $[S]$=$\{[v], \mathcal{F}\}$ given reference sketch-image pair(s), users can provide a blending mask M_B and a part sketch inside the mask to indicate an editing input. Then, our method blends the local sketch with the original sketch to be an edited sketch S fed into the learned dual-encoder $\mathcal{F}$. Given the extracted sketch feature and a prompt *"a photo of a* $[v]$*"*, the denoising U-Net produces a foreground latent, which is blended with the background latent inverted from the original image via M_B, to achieve the final editing result. The two latents are blended during all the inference time steps (T=50). Figure 15 presents more local editing results for human portrait manipulation (Top) and virtual try-on/clothing design (Bottom).

Concept Transfer. Our method can transfer the learned concepts locally or globally to a target object with similar semantics, as shown in Figure 16. Similar to the pipeline of local editing (Figure 14), users may provide an editing input to indicate local shape or structure to transfer a target concept $[S]$.

Multi-concept Generation. Given a set of the extracted sketch concepts $\{S_i\}$=$\{[v_i], \mathcal{F}_i\}$, our method can directly combine them without extra optimization. Figure 17 shows the pipeline of multi-concept generation implemented by our method. Given an input sketch annotated with diverse concepts, our method divides it into separate sketches fed

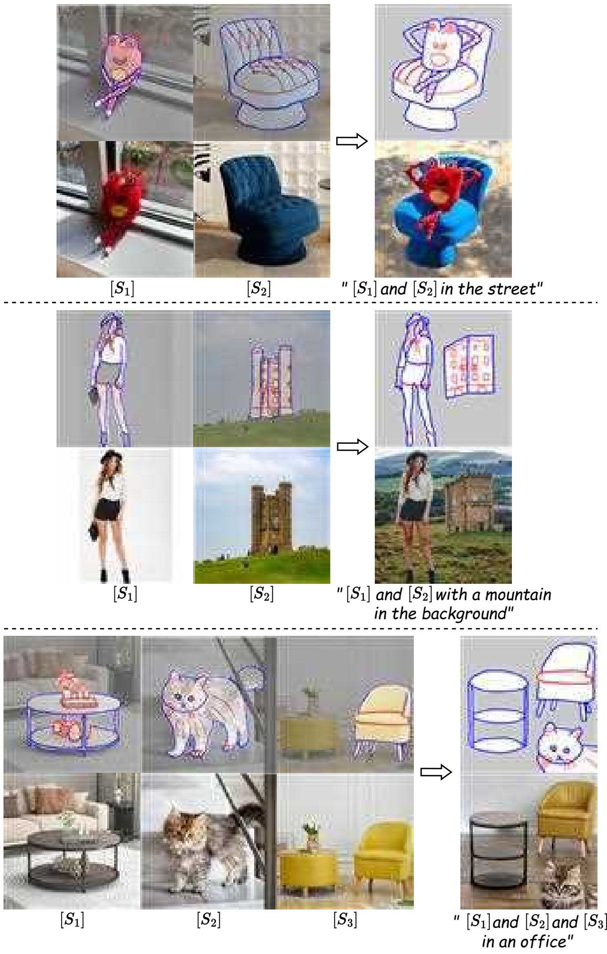
[S_1]
[S_2]
" [S_1] and [S_2] in the street"
[S_1]
[S_2]
" [S_1] and [S_2] with a mountain in the background"
[S_1]
[S_2]
[S_3]
" [S_1] and [S_2] and [S_3] in an office"

Figure 13. Additional results of multi-concept generation enabled by our method. The prefix of the text prompt is *"a photo of ..."*.

into their corresponding dual-encoder F_i. Then, the extracted features are masked respectively using M_i and then aggregated together by summation, finally injected into the pre-trained T2I diffusion model. The given prompt is in the format of "$[v_1]$ and $[v_2]$ ... and $[v_i]$" to cover multiple concepts. Figure 13 shows more results of multi-concept generation.

Text-based Style Variation. Our method decouples global semantics and local features of a reference image to a textual token $[v]$ and a sketch encoder $\mathcal{F}$. Thus, our method can be used to produce diverse style variations of the target object while preserving its geometry (shape and details), as shown in Figure 18. To this end, our method first extracts a concept $[S]$=$\{[v], \mathcal{F}\}$ from sketch-image pair(s). Then, it takes as input the sketch (regarded as an intermediate representation of object geometry) fed to $\mathcal{F}$ and a style prompt without the learned $[v]$ from the original image (e.g., "a crayon drawing") to control the target style. We compared our method with PnP [54], a text-based image-to-image translation method, by feeding a masked image (only with a foreground object) to this method. PnP consists of an inversion step and an inference step. For comparison, we provided an initial prompt (e.g., "a photo of a toy" for the toy category) for inversion and a style prompt (e.g., "a crayon drawing of a toy") for inference to change the object style. Thanks to the given sketch, our method better disentangles the geometry and style, thus offering more user controllability and flexibility via sketching.

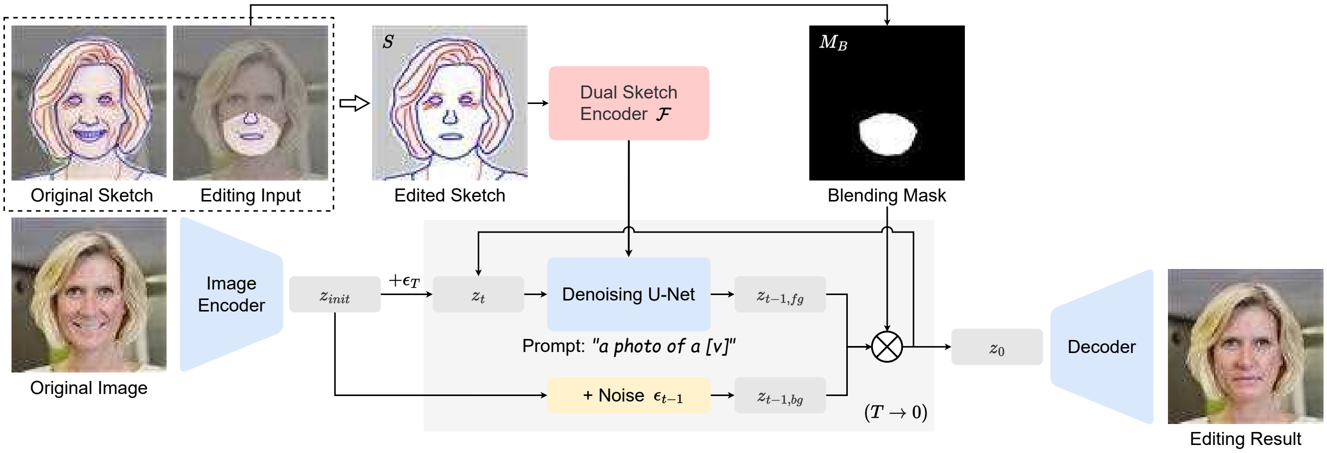

Figure 14. The pipeline of local editing enabled by our method.

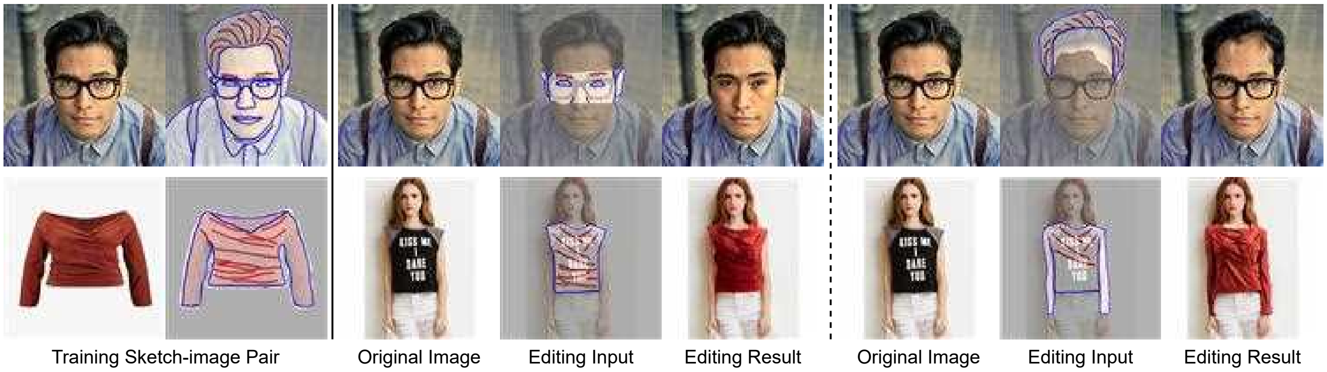

Figure 15. Additional results of local editing enabled by our method. The top row is for human portrait manipulation (removing the glasses and changing the hair region), while the bottom row is for virtual try-on and clothing design.

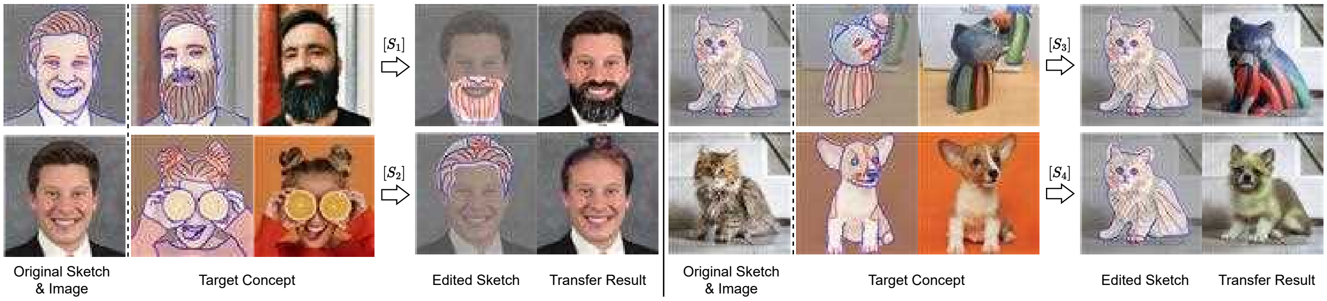

Figure 16. Additional results of concept transfer enabled by our method. The left half shows examples of local concept transfer for adding a beard (Top) and adding a hair bun (Bottom). The right half shows examples of global concept transfer for changing the object semantics while preserving its shape and pose.

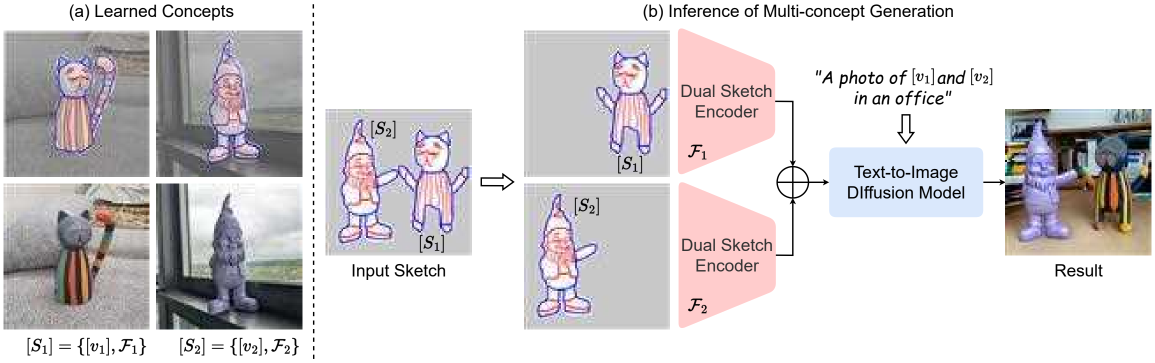
(a) Learned Concepts
$[S_1] = \{[v_1], \mathcal{F}_1\}$
$[S_2] = \{[v_2], \mathcal{F}_2\}$
(b) Inference of Multi-concept Generation
$[S_2]$
$[S_1]$
Input Sketch
Dual Sketch Encoder
$\mathcal{F}_1$
$\mathcal{F}_2$
"A photo of $[v_1]$ and $[v_2]$ in an office"
Text-to-Image DIffusion Model
Result

Figure 17. The pipeline of multi-concept generation enabled by our method. Separately learning each concept (a), our method can directly combine them for multi-concept generation during inference (b) without extra fine-tuning.

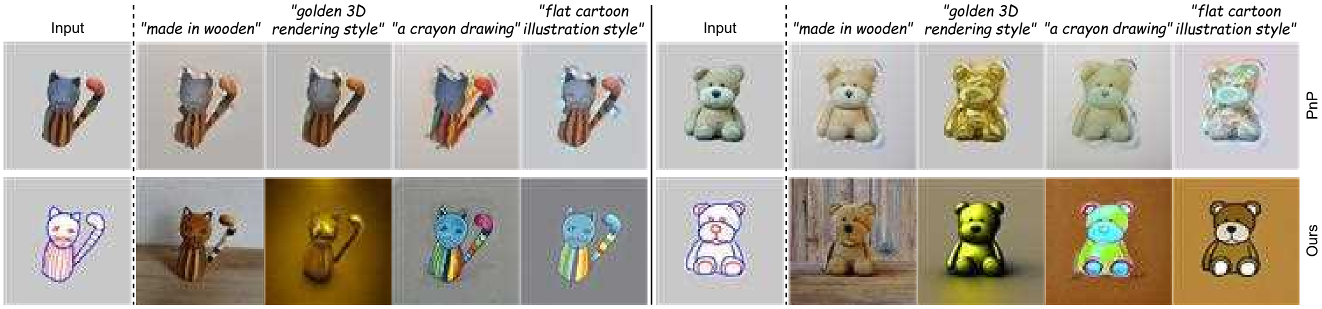
Input
"made in wooden"
"golden 3D rendering style"
"a crayon drawing"
"flat cartoon illustration style"
Input
"made in wooden"
"golden 3D rendering style"
"a crayon drawing"
"flat cartoon illustration style"
PnP
Ours

Figure 18. Comparisons of the results by our method and PnP [54] for text-based style variation.

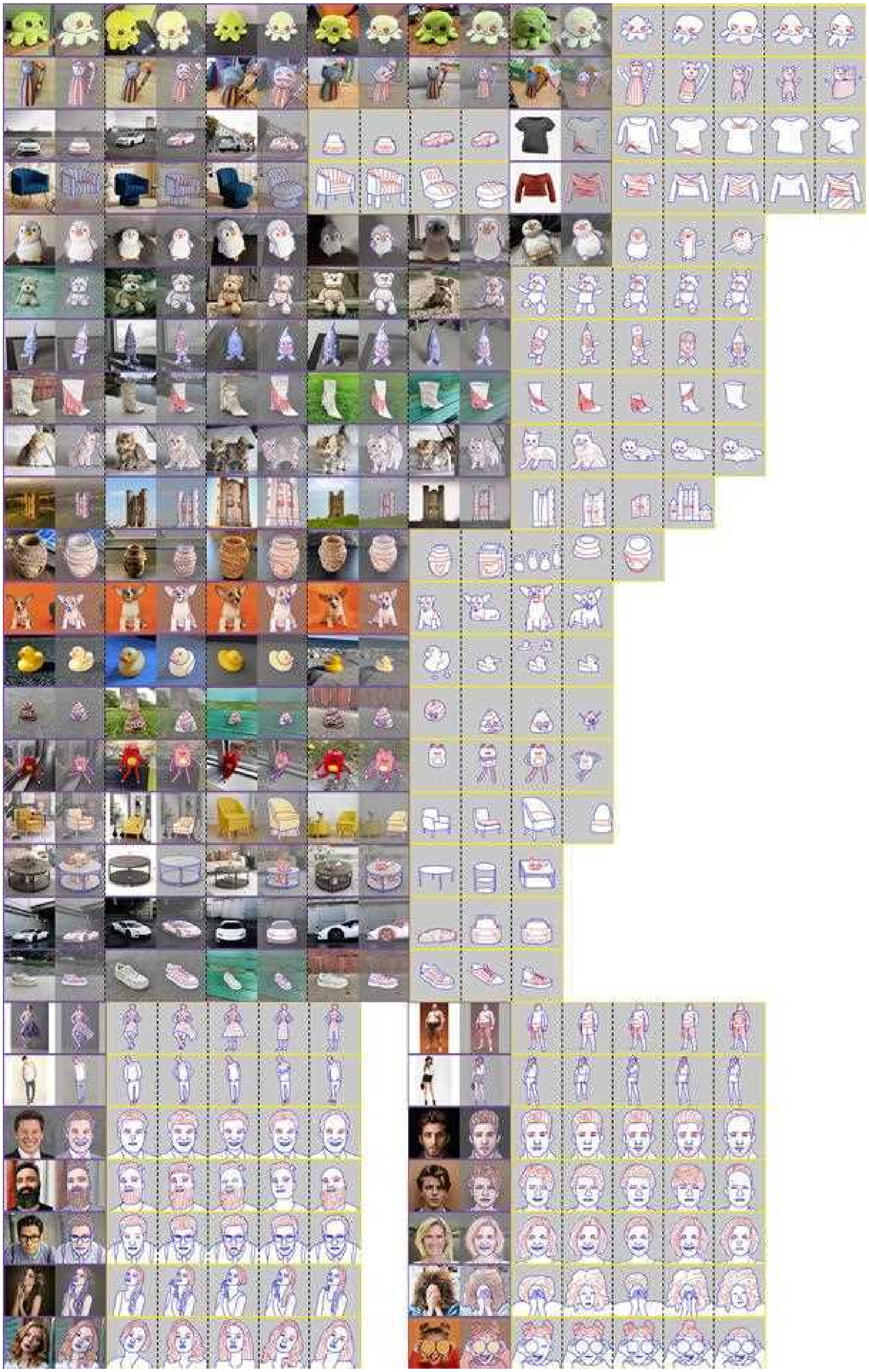

Figure 19. A thumbnail of our created dataset for training and testing. The pairs of reference images and the corresponding traced sketches are with purple borders, while the edited sketches are with yellow borders.

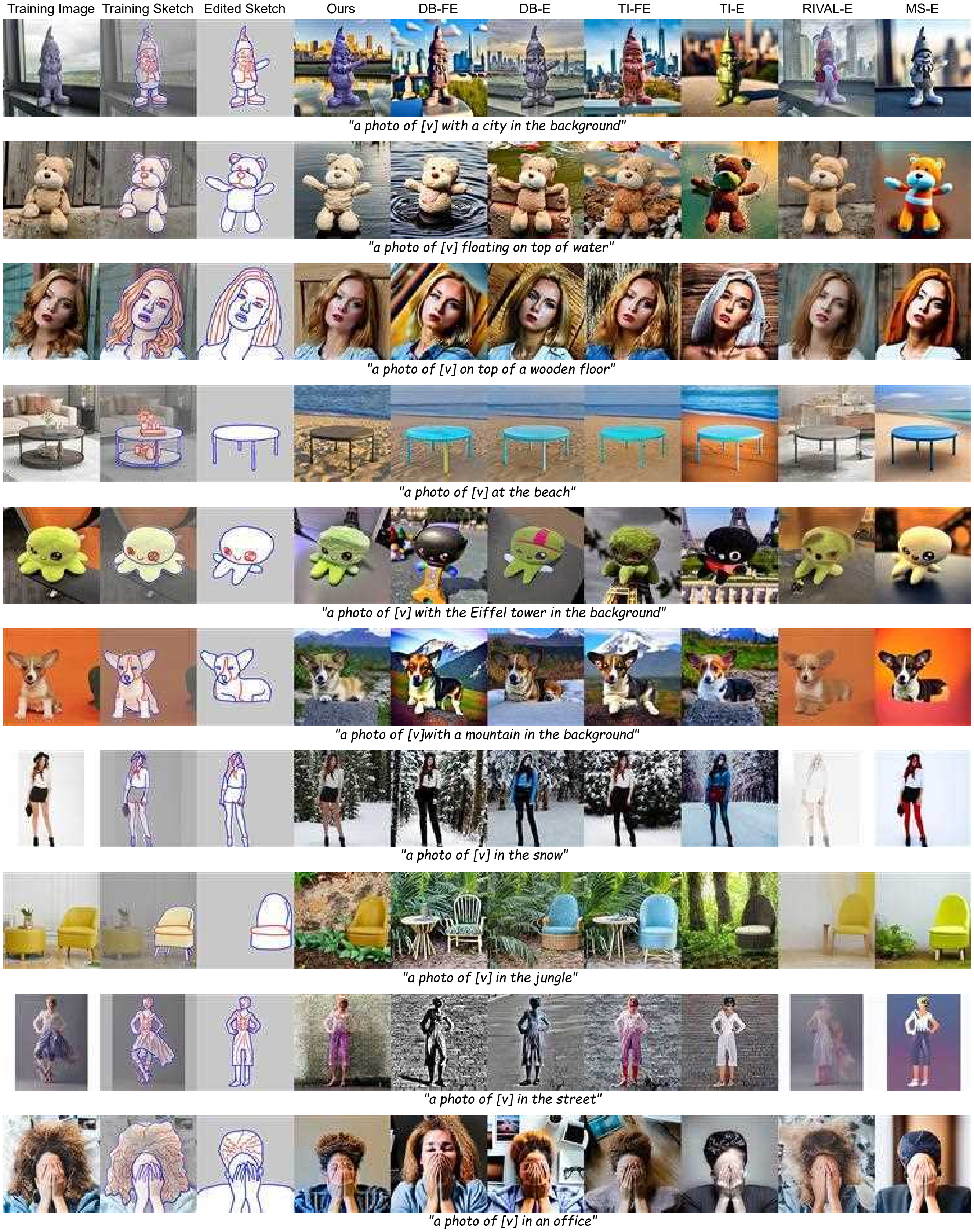
Training Image
Training Sketch
Edited Sketch
Ours
DB-FE
DB-E
TI-FE
TI-E
RIVAL-E
MS-E
"a photo of [v] with a city in the background"
"a photo of [v] floating on top of water"
"a photo of [v] on top of a wooden floor"
"a photo of [v] at the beach"
"a photo of [v] with the Eiffel tower in the background"
"a photo of [v]with a mountain in the background"
"a photo of [v] in the snow"
"a photo of [v] in the jungle"
"a photo of [v] in the street"
"a photo of [v] in an office"

Figure 20. Comparisons of the results generated by our method and the adapted state-of-the-art methods, given the same training data (sketch-image pairs in Columns 1 & 2), edited sketch (Column 3), and text prompt (at the bottom of each group of results).

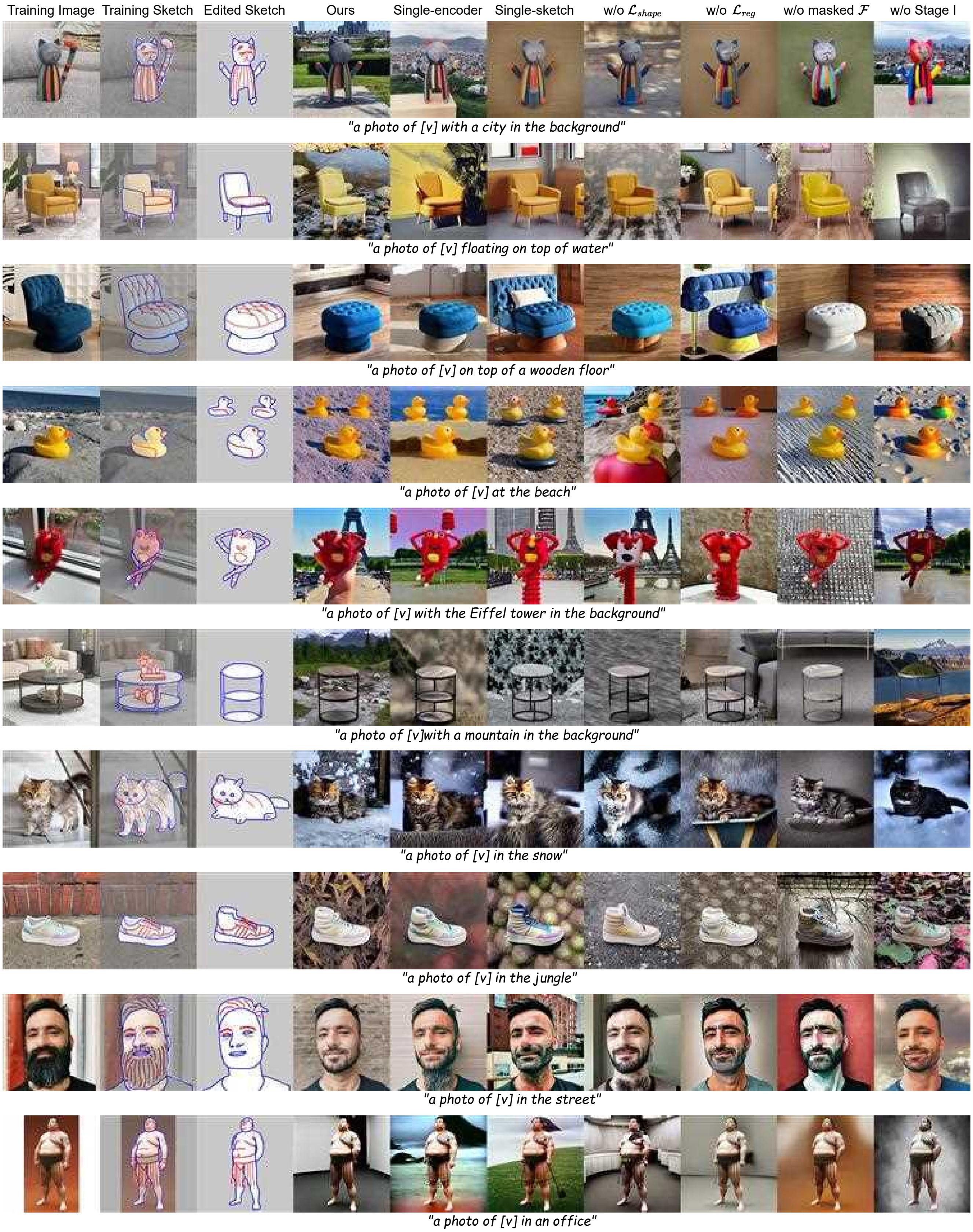
Training Image
Training Sketch
Edited Sketch
Ours
Single-encoder
Single-sketch
w/o $\mathcal{L}_{shape}$
w/o $\mathcal{L}_{reg}$
w/o masked $\mathcal{F}$
w/o Stage I
"a photo of [v] with a city in the background"
"a photo of [v] floating on top of water"
"a photo of [v] on top of a wooden floor"
"a photo of [v] at the beach"
"a photo of [v] with the Eiffel tower in the background"
"a photo of [v]with a mountain in the background"
"a photo of [v] in the snow"
"a photo of [v] in the jungle"
"a photo of [v] in the street"
"a photo of [v] in an office"

Figure 21. Comparisons of the results generated by our method and the ablated variants, given the same training data (sketch-image pairs in Columns 1 & 2), edited sketch (Column 3), and text prompt (at the bottom of each group of results).